

SUPPORTING INFORMATION

Modular amphiphilic poly(aryl ether)-based supramolecular nanomicelles:

An efficient endocytic drug carrier

Ramya Kannan,^{1,2} Ayan Datta,¹ Palani Prabakaran,¹ Edamana Prasad,^{1} and Vignesh*

Muthuvijayan^{2}*

¹Department of Chemistry, Indian Institute of Technology Madras, Chennai, India

²Department of Biotechnology, Bhupat and Jyoti Mehta School of Biosciences, Indian

Institute of Technology Madras, Chennai, India

Author Email Address: pre@iitm.ac.in ; vigneshm@iitm.ac.in

Table of contents:

S.No	Figure captions	Page No
1.	Schemes S1 – S4: Synthesis of compounds D1 and D2	2 – 5
2.	Experimental Section	5-10
3.	Figures S5 – S10: ¹ H, ¹³ C and Mass spectra of D1 and D2	10-13
4.	Table S11: Gelation of compounds D1 and D2 and their critical gel concentration (CGCs) values	13
5.	Figure S12: SEM images of a-b) D1 (1 wt %) and c-d) D2 (1 wt %) in DMSO: water (2:8 v/v)	14
6.	Figure S13: Strain and frequency sweep measurements of a) D1 gel and b) D2 gel in DMSO: water (2: 8 v/v)	14
7.	Figure S14. Critical micellar concentration of D1 and D2	15

8.	Figure S15: Aggregation of the amphiphilic dendrimers D1 and D2 (50 and 10 μ M) in PBS for 96 h	15
9.	Figure S16: Small angle and wide angle X-ray diffraction patterns of (a) D1 and (b) D2 in DMSO: water (2:8 v/v)	16
10.	Figure S17. Variable temperature NMR spectra of D1 in DMSO- d_6 from 30 $^{\circ}$ C to 100 $^{\circ}$ C	16
11.	Figure S18. Variable temperature NMR spectra of D2 in DMSO- d_6 from 30 $^{\circ}$ C to 100 $^{\circ}$ C.	17
12.	Table S19. Entrapment and loading efficiency of D2 nanomicelles with doxorubicin	17
13.	Table S20. Results and the equation parameters of the drug release kinetics of Doxorubicin from D2-Dox	18
14.	Figure S21: Flowcytometric analysis of the D2-Dox and Dox on a) NIH/3T3 cells incubated for 4 h; b) Mean fluorescence intensity of the internalized D2-Dox and free Dox in NIH/3T3 cells for 4 h	18
13.	References	19

Experimental section

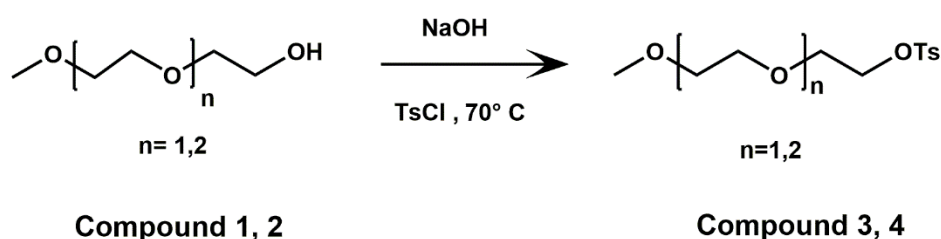
Materials

3,4,5-trihydroxy benzoate was purchased from Sigma-Aldrich. Potassium carbonate and hydrazine monohydrate were purchased from Fischer scientific. 2-(2-methoxyethoxy) ethanol, 2-(2-(2-methoxyethoxy)ethoxy) ethanol, tetrabutyl ammonium iodide and p-toluenesulfonyl chloride (TsCl) were purchased from spectrochem. $CDCl_3$ was purchased from Cambridge isotope laboratories, USA. All the starting materials were used as received unless otherwise mentioned. The organic solvents were dried using standard procedure.

Instruments

^1H and ^{13}C NMR data were recorded on Bruker 400 MHz spectrometer in CDCl_3 and DMSO-d_6 solvent. High resolution mass spectra (HRMS) were recorded using Micromass Q-TOF mass spectrometer. The morphology of the gels and nanoparticles were examined using scanning electron microscopy (SEM) (FEI quanta FEG 400). TEM measurements were carried out using High resolution Transmission electron microscopy (HR-TEM) JEOL 3010. Size measurements of the dendrimer nanoparticles were carried out using Malvern Zetasizer ZS90 at 25 °C. Fluorescence measurements were conducted with Horiba Jobin Yvon Fluoromax-4 fluorescence spectrophotometer. Fluorescence imaging was performed using the Olympus inverted fluorescence microscope (Model IX73, Japan). Powder-XRD pattern were recorded on Bruker D8 Advance X-ray diffractometer using $\text{Cu-K}\alpha$ radiation ($\lambda = 1.542 \text{ \AA}$). UV-visible spectra were recorded using JASCO V-660 spectrophotometer. Rheology experiments were carried out with Anton Paar MCR-301 rheometer. Absorbance for MTT assay was measured in Bio Rad X-MARK microplate spectrophotometer. Flow cytometry analysis was done with BD FACS Aria III.

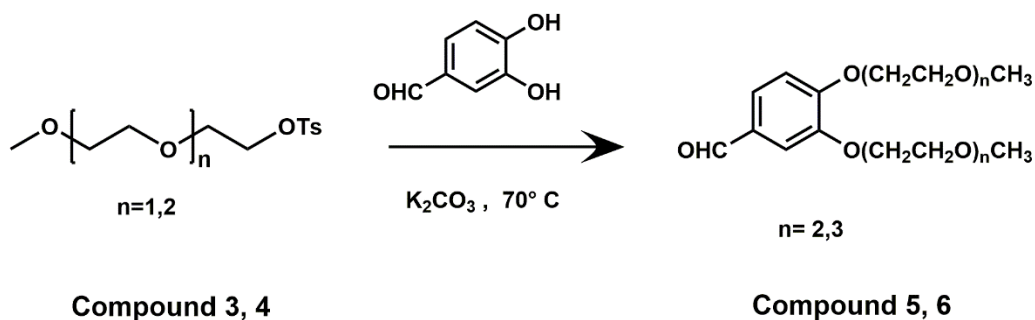
Scheme S1: Synthetic procedure of compounds 3 and 4



Scheme S1. Synthesis of Compounds 3 and 4

Compound 1 (2-(2-Methoxyethoxy)ethyl alcohol) (25 mL, 0.2 mole) in 50 mL of THF was added drop wise to a solution of NaOH (12.2 gm, 0.3 mol) in water and THF (45 mL) at 0 °C. This mixture was stirred for further 30 minutes before the drop wise addition of p-toluenesulfonyl chloride (tosyl chloride) (35 g, 0.18 mol) in 50 mL of THF. After being stirred at 70 °C for 2 hours, the mixture was poured onto ice-cold water. This solution was extracted in dichloromethane that was subsequently dried with sodium sulphate, and all volatile materials were removed by rotary evaporation, yielding colorless oil (compound 3) with 80% yield. Similar procedure was performed for compound 4 synthesis from compound 2 (2-(2-(2-Methoxyethoxy)ethoxy) ethyl alcohol) which resulted with an 80 % yield.

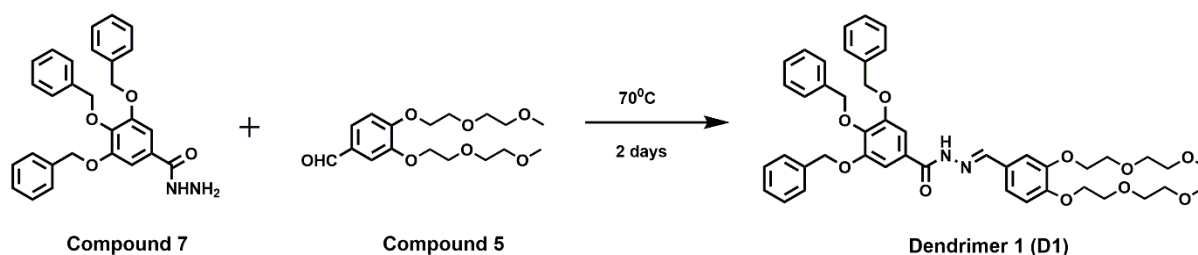
Scheme S2: Synthetic procedure of compounds 5 and 6



Scheme S2. Synthesis of compounds 5 and 6

3,4-dihydroxy benzaldehyde (2 gm, 0.014 mole), compound 3 (8.74 gm, 0.032 mole) and potassium carbonate (6 gm, 0.043 mole) were taken in 30 mL of DMF as a solvent in a 100 mL of round bottom flask and refluxed in 70 °C for 24 hours. The solvent was removed under reduced pressure using a rotary evaporator and the solid was taken in ethyl acetate and washed with water for several times and the organic layer was dried over Na₂SO₄. The organic solvent was removed under reduced pressure to afford oil as product which was purified by column chromatography using silica gel as stationary phase and 3% MeOH in CH₂Cl₂ as eluent to get pure product. The yield of the compound 5 was 80%. Similar procedure for the synthesis of compound 6 was carried out with compound 4, under same experimental conditions.

Scheme S3: Synthetic procedure of Dendrimer D1

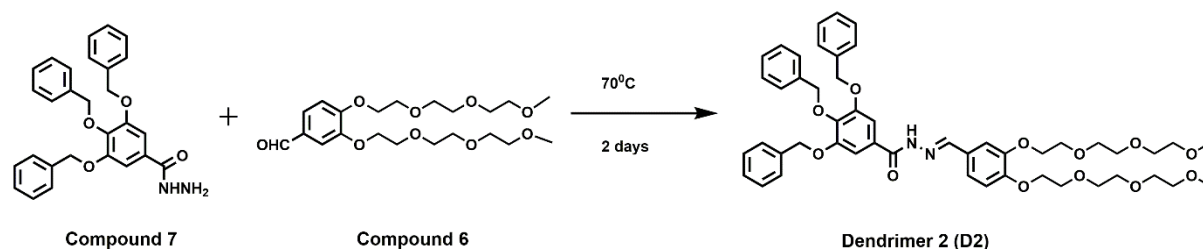


Scheme S4. Synthesis of compound D1

Compound 7 was synthesized according to our reported procedure.¹ 0.5 gm, 0.0011 mole of compound 7 and compound 5 (0.4147 gm, 0.0012 mole) were taken in a 100 mL round bottom flask with 20 mL of MeOH and 20 mL of CHCl₃ as solvent. The solution was refluxed for 48 h. The solvent was evaporated under reduced pressure to get a solid compound which was purified by column chromatography using silica gel as stationary phase and 3% MeOH in CH₂Cl₂ as eluent to afford a pure white product having yield of 90%. **¹H NMR (500 MHz, DMSO-D₆) δ:** 11.66(s, NH, 1H), 8.4(s, N=CH, 1H), 7.5-7(m, Ar-Hs, 20H), 5.2(s, H), 4H), 5(s,

2H), 4.1-3.4(s,CH₂, 16H), 3.25(s,OCH₃,6H). ¹³C NMR (100 MHz, DMSO-D₆) δ:162.28, 152.08, 148.5, 140.04, 137.42, 136.8, 128.46,128.19,128.08, 127.97,127.89,127.7,127.31, 113.48, 110.89, 106.85, 74.29, 71.33, 70.47, 69.83, 68.91,68.85,68.36,68.24, 58.08. HRMS (ES⁺): m/z Calculated for C₄₅H₅₁N₂O₁₀:779.3544, found: 779.3563 [M⁺H]⁺.

Scheme S4: Synthetic procedure of Dendrimer D2



Scheme S5. Synthesis of compound D2

Compound 7 (0.5 gm, 0.0011 mole) and compound 6 (0.616 gm, 0.0014 mole) were taken in a 100 mL round bottom flask with 20 mL of MeOH and 20 mL of CHCl₃ as solvent. The solution was refluxed for 48 hours. The solvent was evaporated under reduced pressure to get a solid compound which was purified by column chromatography using silica gel as stationary phase and 3% MeOH in CH₂Cl₂ as eluent to afford a pure white compound as product. The yield of the compound was 91%. ¹H NMR (500 MHz, DMSO-D₆) δ: 11.63(s, NH,1H), 8.4(s, N=CH, 1H), 7.5-7(m, Ar-H,20H), 5.2(s, H), 4H), 5.02(s, Ar-H, 2H), 4.15-3.5(s,CH₂,16H), 3.4(s,OCH₃,6H). ¹³C NMR (100 MHz, DMSO-D₆) δ:162.28, 152.08, 150.33, 148.5, 147.96, 140.04, 137.42, 136.8, 128.76,128.47,128.19, 128.09, 127.97,127.89,127.7,127.33, 121.93, 113.54, 110.92, 106.88, 74.29, 71.3, 70.5, 70.04, 69.85, 69.61,68.94,68.88,68.37,68.26, 58.04. HRMS (ES⁺): m/z Calculated for C₄₉H₅₈N₂O₁₂:889.3887, found: 889.3857 [M⁺H]⁺.

Methodology:

Gelation and aggregation of amphiphilic dendrimers: Gelation of the two dendrimers **D1** and **D2** in different solvents and solvent mixtures was characterized by the vial inversion method. Furthermore, the critical micellar concentration of **D1** and **D2** was also measured by the pyrene probe method. The pyrene emission fluorescence spectrum was recorded on a Horiba Fluoromax spectrometer. Pyrene was used as the fluorescent probe to determine the critical micelle concentrations (CMCs) of the amphiphilic dendrimers. Pyrene stock solution of 50 μM in acetonitrile was freshly prepared. 5 μM of pyrene solution was then added to different vials containing 10 mL of PBS buffer (pH.7.4). To this aqueous solution, increasing

concentrations (0.5-50 μM) of dendrimer amphiphiles (**D1** and **D2**) were added, vortexed, and stirred for 4 h at room temperature in dark. Fluorescence spectra of the samples were collected at 25 °C with an excitation at 334 nm, slit width of 2 nm. The emission intensity band at 372 and 392 nm were determined, and then a plot of ratio of the intensities versus the logarithm of the amphiphilic dendrimer concentration was plotted. A linear regression of the two straight lines were performed and the critical micellar concentration (cmc) was determined to be the point of intersection of the independent linear regressions.

Nanomicelles preparation by Film hydration Method:

Nano-sized assemblies of the dendrimers were formed by the film hydration method. Briefly, the **D1** and **D2** dendrimer (5 mg) was dissolved in 10 mL ethanol. The solvent was removed by vacuum rotary evaporation to form a dry film. The dried film was then hydrated with 10 mL PBS buffer (pH 7.4) at 60 °C for 30 minutes under stirring. The dendrimer containing aqueous suspension was then sonicated for 30 minutes, to completely remove any excess solvent.

Physicochemical characterization of the dendrimer gels and micelles:

The formed self-assembled structures were visualized by the Scanning Electron Microscopy (SEM) and Transmission Electron Microscopy (TEM). The particle size of the aggregates was measured by Dynamic Light Scattering (DLS). To understand the mechanical properties of the gel, the strain and frequency sweep measurements using 1.0 wt% of the gel was recorded using a rheometer. These rheology experiments were carried out with an Anton Paar MCR-301 rheometer. A parallel plate of 25 mm was used for the measurement. The storage modulus (G') and loss modulus (G'') were measured as functions of strain and frequency. The molecular packing of the amphiphilic dendrimers was analyzed by powder XRD and temperature dependent NMR measurements. Powder-XRD patterns were recorded on the Bruker D8 Advance X-ray diffractometer using Cu- K_{α} radiation ($\lambda = 1.542 \text{ \AA}$).

Doxorubicin loading in D2 nanomicelles (D2-Dox):

10 mg of **D2** dendrimer dissolved in 10 mL of ethanol was dried using a roto evaporator to form a thin film. To this, PBS buffer solutions containing doxorubicin (5-30 mg) at different mass ratios (1:2, 1:1, 2:1, and 1: 3) were added and sonicated for 30 minutes. Unentrapped doxorubicin was separated by centrifugation (10,000 rpm) for 30 minutes. The entrapment efficiency (EE) and drug loading (DL) for the Dox-loaded **D2** (D2-Dox) were measured by quantifying the absorbance using the UV-vis spectrophotometer.

$$\text{Entrapment efficiency \%} = \left(\frac{\text{weight of the actual drug in nanoparticles}}{\text{weight of total amount of drug loaded}} \right) \times 100$$

$$\text{Drug loading \%} = \left(\frac{\text{weight of the actual drug in nanoparticles}}{\text{weight of nanoparticles}} \right) \times 100$$

***In vitro* drug release kinetics from D2-Dox**

The release of doxorubicin from the Dox-loaded **D2** nanomicelles (D2-Dox) was studied to understand the release kinetics. D2-Dox (2 mL, dox equivalent of 200 µg) was transferred into a dialysis bag (mol. wt. cut-off 4,000 Daltons). Free Dox of 200 µg in PBS was kept as control. The dialysis bags with free Dox and D2-Dox were immersed in a 50 mL of PBS containing beaker. The release kinetics was monitored at 37 °C. At predetermined time intervals, 2 mL of sample was withdrawn and replaced with an equal volume of fresh buffer. The drug release study was performed for 80 h. The amount of Dox released was quantified by measuring the absorbance using UV spectrophotometer. The release experiments were conducted in triplicates and results are expressed as mean ± standard deviation.

Modeling of the release kinetics

The release of Dox from the **D2** nanomicelles were modeled to elucidate the drug release kinetics. Two drug release kinetic models, namely the first order model ² and the Korsmeyer–Peppas model ³ were used to fit the experimental data.

First order model

Gibaldi and Feldman proposed the application of the first order model for drug dissolution kinetics in 1967 ⁴. Pharmaceutical drug carriers which contain water-soluble drugs in a matrix reservoir system are mostly fitted with first order kinetics. The drug release is said to be proportional to the amount of drug in the interior, as the amount of drug released diminishes over time. First order kinetic model equation is also referred to as Noyes-Whitney's equation and is given below as

$$Q_t = Q_0 e^{-kt}$$

Where, Q_t is the amount of drug released at time t , Q_0 is the initial amount of drug, and k is the first order release constant.

Peppas–Korsmeyer model

The Peppas equation was developed by Korsmeyer et al.⁵ and is generally used to analyze the release of pharmaceutical drug from drug carriers when the release mechanism is not well known or when more than one type of release is involved. The equation is given below as

$$\frac{M_t}{M_\infty} = kt^n$$

Where, M_t is the amount of drug released in time t , M_∞ is the amount of drug loaded, k is a rate constant, and n is the diffusional exponent. The drug release mechanism can be predicted based on the n value. The model is valid only for non-degradable delivery systems and is applicable only for the first 60% of drug release. The n value in the equation predicts the mechanism of release based on Fick's law of diffusion. The n value is dependent on the geometry of the drug delivery carrier used.

Cell culture studies

Mouse fibroblasts cells (NIH/3T3), and human breast cancer cells (MCF7) were procured from NCCS, Pune, India for the *in vitro* studies. The cells were cultured in DMEM (Dulbecco's Modified Eagle's Medium) with 10% FBS (Fetal bovine serum) supplemented with 1% penicillin-streptomycin, maintained at 37 °C in a humidified atmosphere containing 5% CO₂. Sub-confluent cells were trypsinized, harvested, counted, and seeded on the well plates for the experiment.

Cytotoxicity of the D2 nanomicelles

The cytotoxicity of the **D2** nanomicelles was assessed by MTT assay based on a previously reported procedure.⁶ The **D2** nanomicelles at different concentrations (0.1-2 mg/mL) were evaluated for their cytotoxicity on both NIH/3T3 and MCF7 cells for 48 h. The cells were incubated with media containing different concentrations of empty **D2** nanomicelles. After the exposure time, the medium was removed and washed with PBS. Further, 100 µl of 10% 3-(4,5-dimethylthiazol-2-yl)-2,5-diphenyltetrazolium bromide (MTT) solution in media was added. The plates were then incubated for 3 h. DMSO was added to dissolve the formazan crystals. The absorbance of the MTT reagent was measured using a Bio-Rad X-MARK microplate spectrophotometer at a wavelength of 570 nm. Each experiment was done in triplicates, and the mean \pm standard deviation was plotted. The viabilities of both NIH/3T3 and MCF7 cells were estimated based on the following equation.

$$\% \text{ Cell viability} = \left(\frac{\text{Mean optical density (OD) of the test samples}}{\text{control samples OD}} \right) \times 100$$

***In vitro* anticancer activity assay**

The antiproliferation activities of the free drug (Dox) and D2-Dox nanomicelles against human breast cancer cells MCF7 and mouse fibroblast cells NIH/3T3 were evaluated by MTT method. The cells (5×10^3 cells/ well) were seeded in 96-well plates and incubated overnight to adhere. The cells were then incubated with either free doxorubicin or D2-Dox nanomicelles for 48 h. After the exposure time, cell viability was measured by the MTT assay. In addition, the IC₅₀ values of the D2-Dox and free Dox were estimated. IC₅₀ value is the half maximal inhibitory concentration, which is a measure of the potency of a substance in causing 50% inhibition of a specific biological or biochemical function *in vitro*. The cell viability % was plotted against concentration, fitted with the linear regression to obtain the IC₅₀ values.

Visualization of cellular uptake

MCF7 cells seeded onto 24-well plates were left overnight for cell attachment. Further, the cells were treated with free Dox and D2-Dox nanomicelles with Dox equivalent 20 µg/mL for 2 h at 37 °C. The treated cells were fixed using 4% formaldehyde for 10 minutes. The cells were then washed thrice to remove the fixative and then stained with Hoechst (nuclei stain). Fluorescence images were taken via an Olympus inverted fluorescence microscope.

Intracellular uptake by flow cytometry analysis

MCF7 and NIH/3T3 cells were seeded in 6 well plates at a density of 1×10^6 cells/well and incubated for 24 h. The cells were then treated with free Dox and D2-Dox nanomicelles (Dox equivalent 20 µg/ml) for 2 h. The treated cells were washed twice with PBS and suspended by addition of trypsin. The cell suspensions were centrifuged at 1500 rpm for 5 min, and the supernatants were discarded. The resulting cell pellets were resuspended in an ice-cold PBS and transferred to flow cytometry sample tubes. The samples were examined using flow cytometer BD Aria III. The results were analyzed using FlowJo software V10.

Endocytic mechanism of D2-Dox nanoaggregates

To investigate the possible endocytosis mechanism of D2-Dox nanomicelles, different endocytosis pathway inhibitors were used on MCF7 cells, along with a control. MCF7 cells were seeded at a density of 1×10^5 cells per well in the 12-well plates and incubated for 24 h. The cells were then washed with PBS twice and incubated with the different endocytosis

inhibitors for 1 h. Chlorpromazine (5 $\mu\text{g/mL}$), an endocytic inhibitor of clathrin-mediated endocytosis, amiloride (0.5 mM), an endocytic inhibitor of macropinocytosis, and genistein (0.05 mM), a caveolae-mediated endocytosis inhibitor were used to understand the endocytosis mechanism. After incubation, the media was removed and replaced with 10% FBS containing DMEM media with free Dox or D2-Dox (Dox equivalent 20 $\mu\text{g/ml}$) for 2 h. Then, the medium was removed and the cells were trypsinized. The pellet was resuspended in ice cold PBS solution. The cells were then analyzed by flow cytometry.

Statistical analysis: The values are expressed as mean \pm standard deviation, and statistical analysis was performed using paired t-test by Prism (GraphPad software, version 5.0). The p-values * $p < 0.05$, ** $p < 0.01$, were considered statistically significant

Characterization:

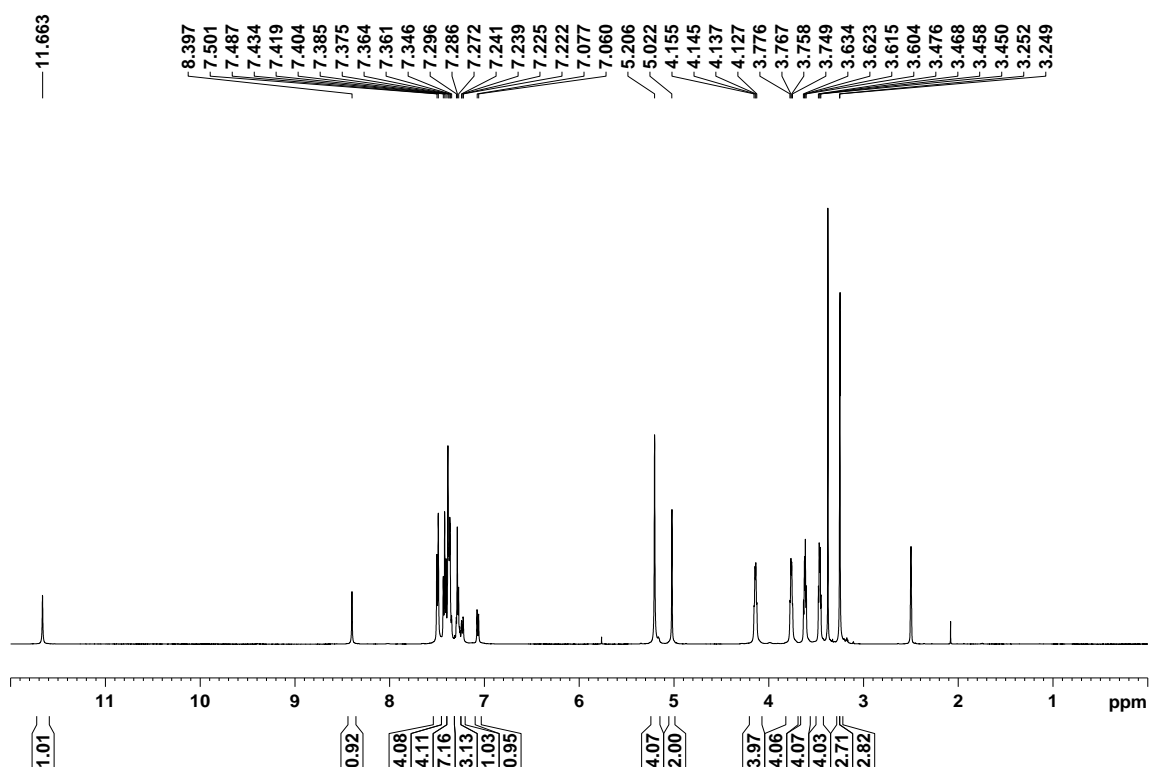


Figure S5: ^1H NMR spectrum of compound D1 in $\text{DMSO-}d_6$.

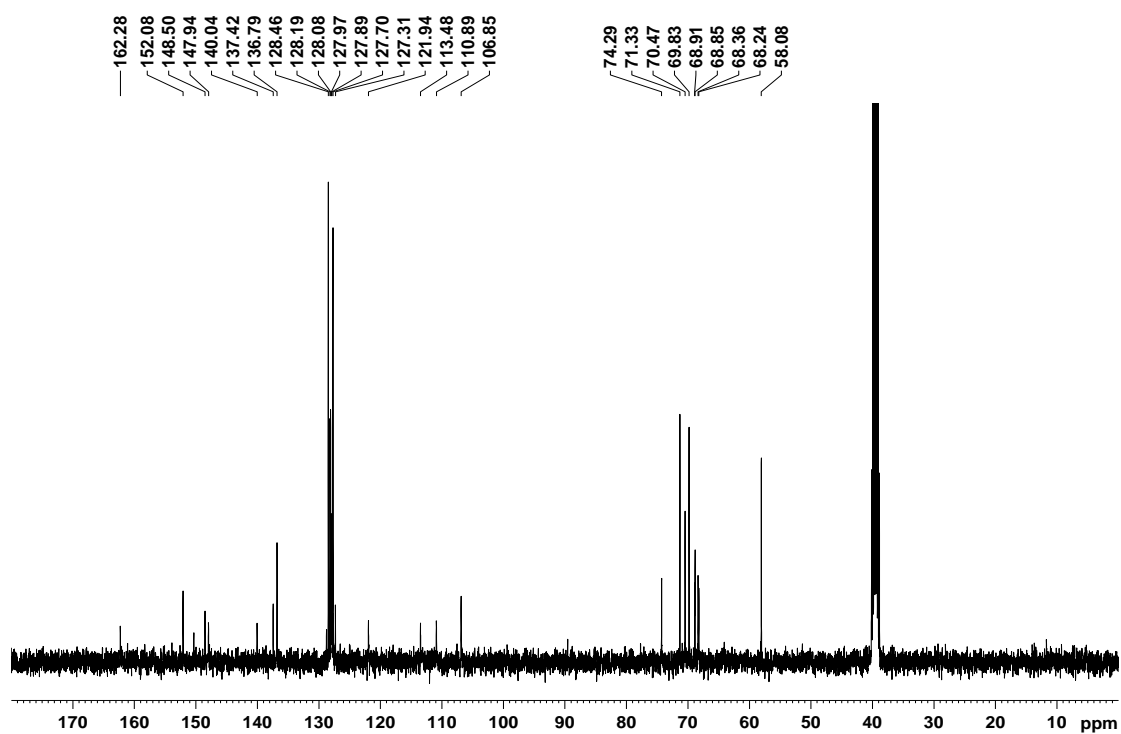


Figure S6: ^{13}C NMR spectrum of compound D1 in DMSO-D_6 .

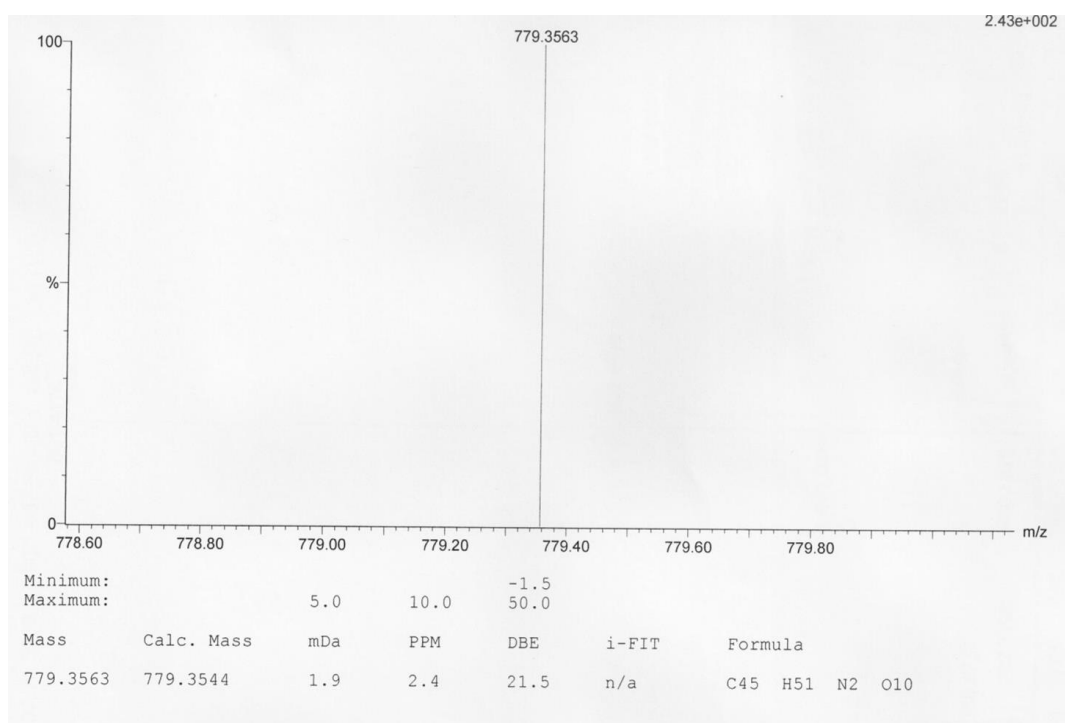


Figure S7. ESI-Mass Spectra of D1

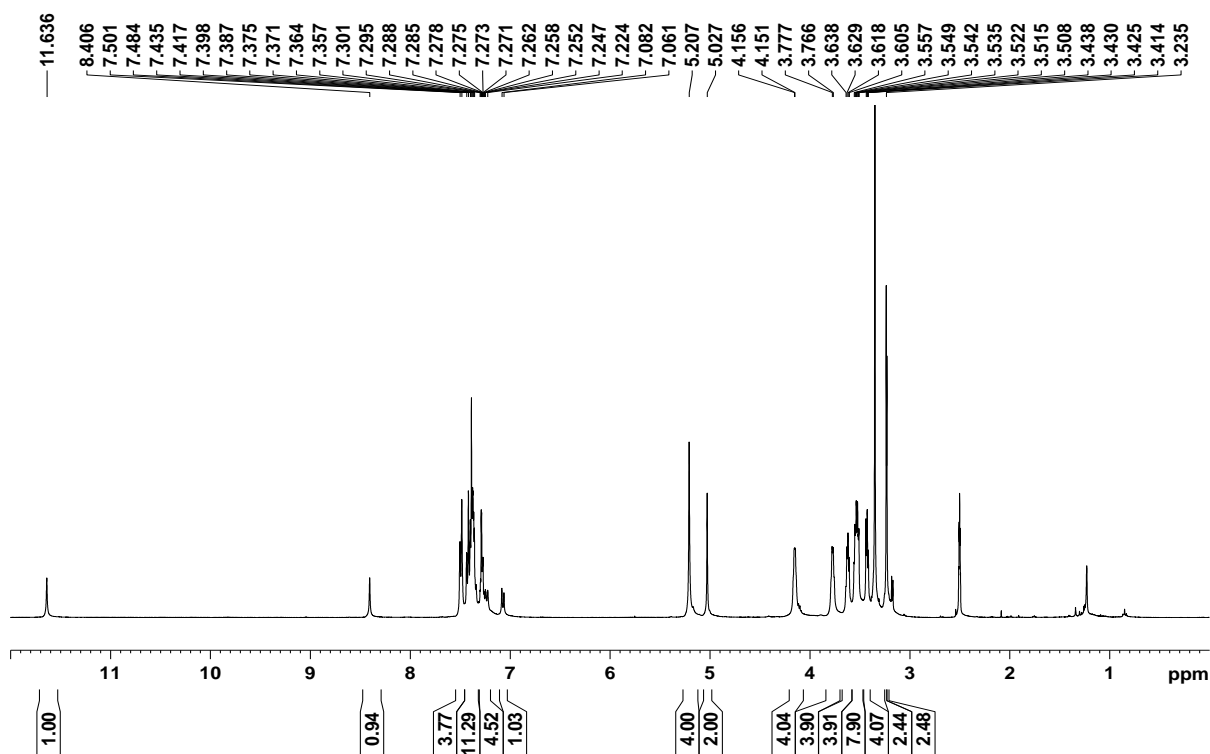


Figure S8. ^1H NMR spectrum of compound D2 in DMSO-D_6

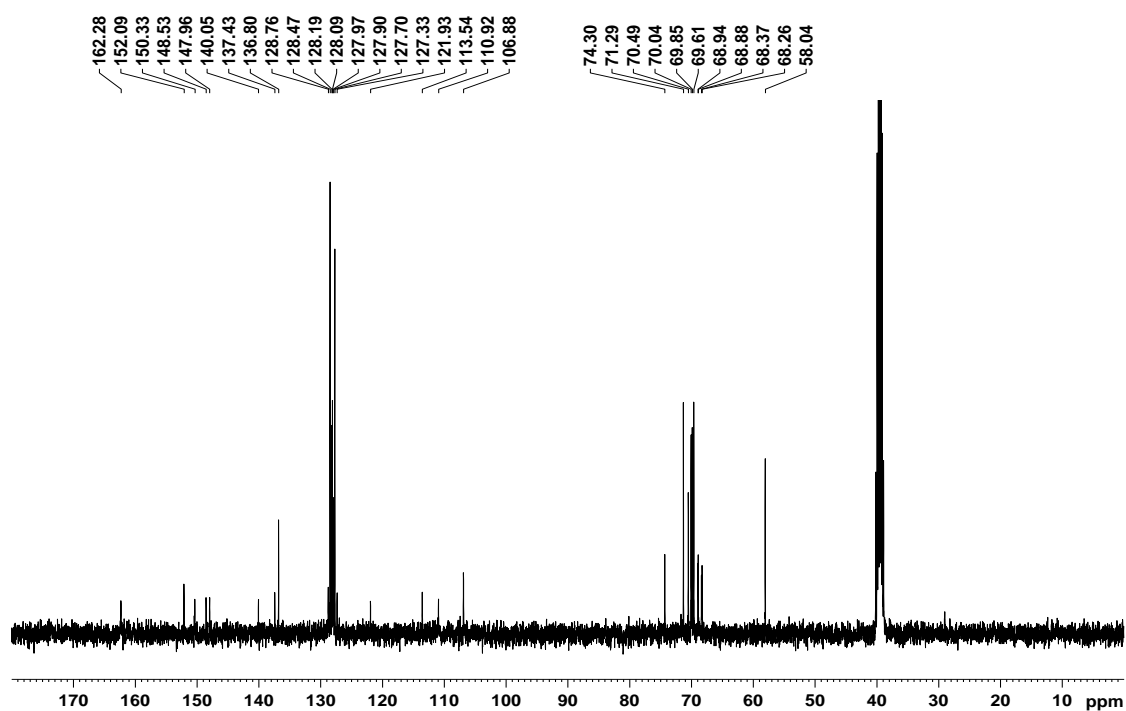


Figure S9. ^{13}C NMR spectrum of compound D2 in DMSO-D_6

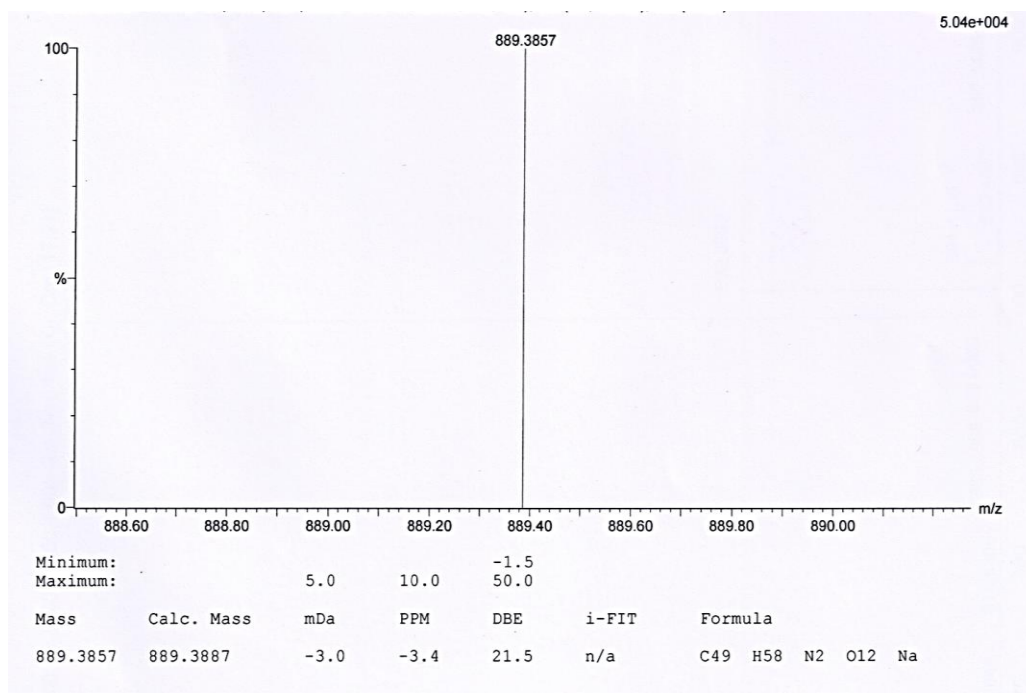


Figure S10. ESI-Mass spectra of compound D2

Table S11. Gelation properties and critical gel concentrations (CGCs) of dendrimers D1 and D2 in different solvents

Solvent	D1	D2
Water	I	I
Hexane	I	I
DMSO	S	S
Ethanol	S	S
Acetone: water (2:8)	G (3 mg/mL)	G (6 mg/mL)
DMSO: water (2:8)	G (4 mg/mL)	G (7 mg/mL)
Ethanol: water (2:8)	G (4 mg/mL)	G (8 mg/mL)
Methanol: water (2:8)	G (6 mg/mL)	PG
Dioxane: water (2:8)	G (7 mg/mL)	PG
Acetonitrile: water (2:8)	PG	PG
S = Solution, G = Gel, PG = Partial gel, I = Insoluble		

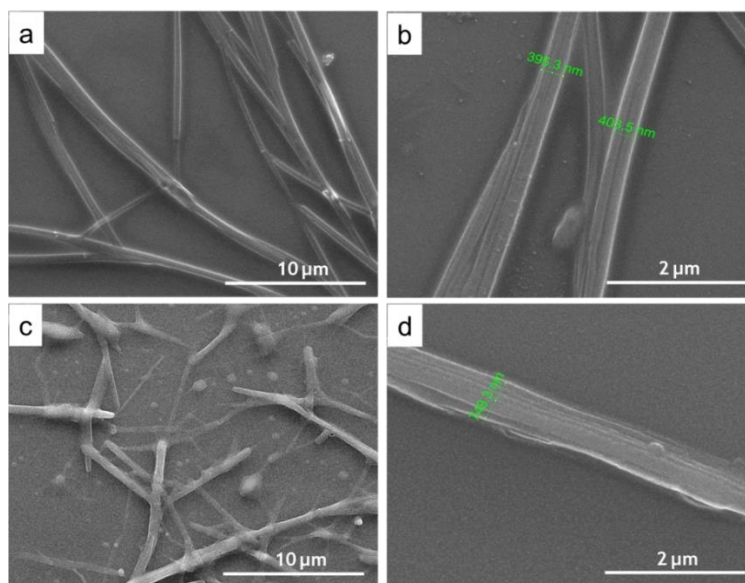


Figure S12. SEM images of a-b) D1 (1 wt %) and c-d) D2 (1 wt %) in DMSO: water (2:8 v/v), indicating a fibrous morphology of the dendrimer gels. The fiber diameter was measured to be ~ 400 – 800 nm for D1 and D2 gels respectively.

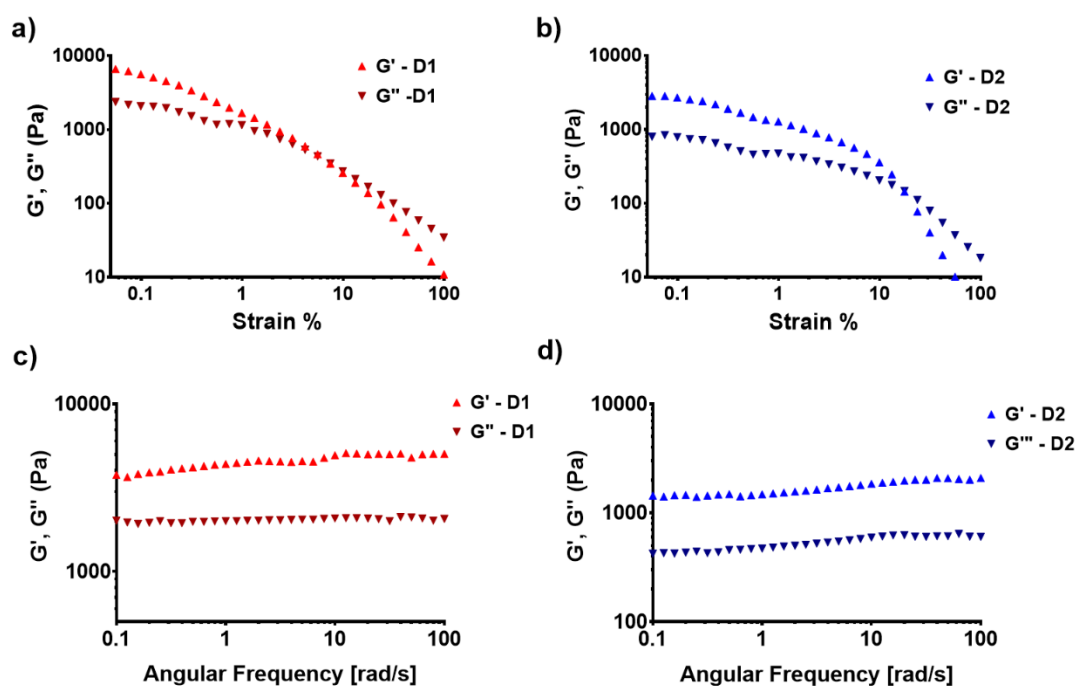


Figure S13. Strain sweep measurements of a) D1 gel and b) D2 gel in DMSO: water (2: 8 v/v) and frequency sweep measurements of c) D1 and d) D2 in DMSO; water (2:8 v/v); G' was found to be always higher than the G'' for both the gels. Frequency independent nature was also observed for both the gels.

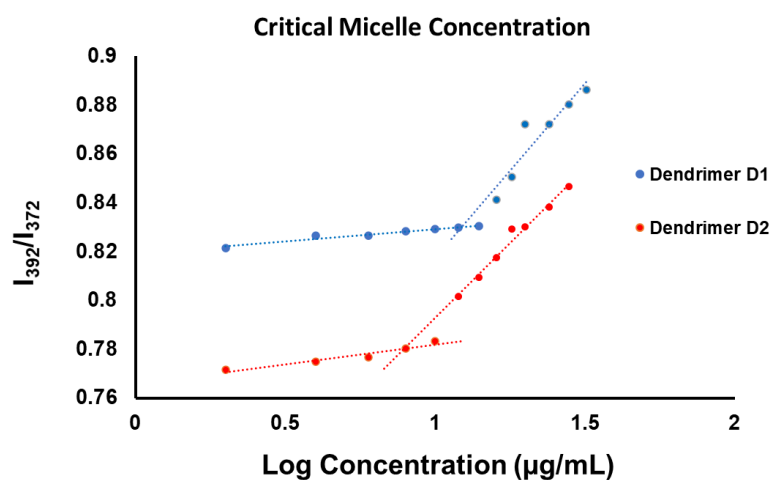


Figure S14. Critical micellar concentration of D1 and D2 (2-20 $\mu\text{g/mL}$) measured by the fluorescence intensity (I_{392}/I_{372}) using the pyrene probe method

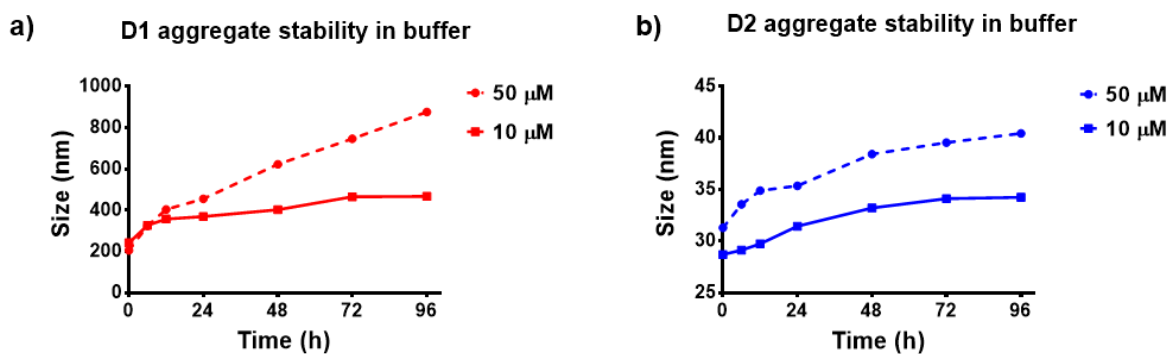


Figure S15. Aggregation of the amphiphilic dendrimers D1 and D2 (50 and 10 μM) in PBS for 96 h measured using Dynamic light Scattering (DLS)

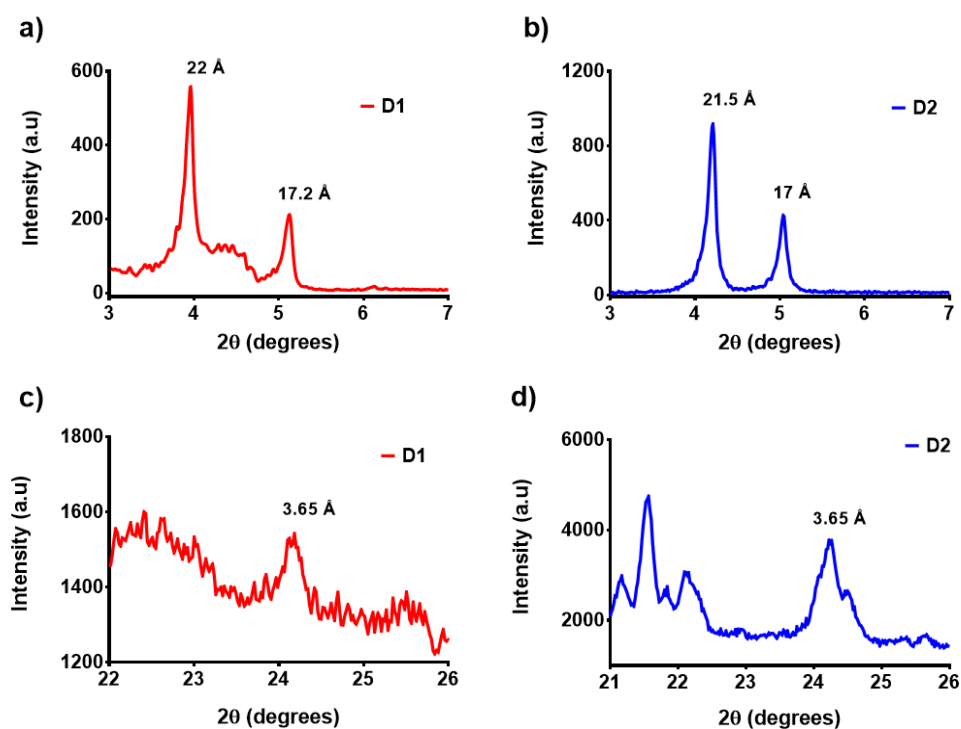


Figure S16. Small angle X-ray diffraction patterns of (a) D1 and (b) D2 in DMSO: water mixture (2:8 v/v) and the wide-angle X-ray diffraction peak of c) D1 and d) D2 depicting the intermolecular π - π stacking

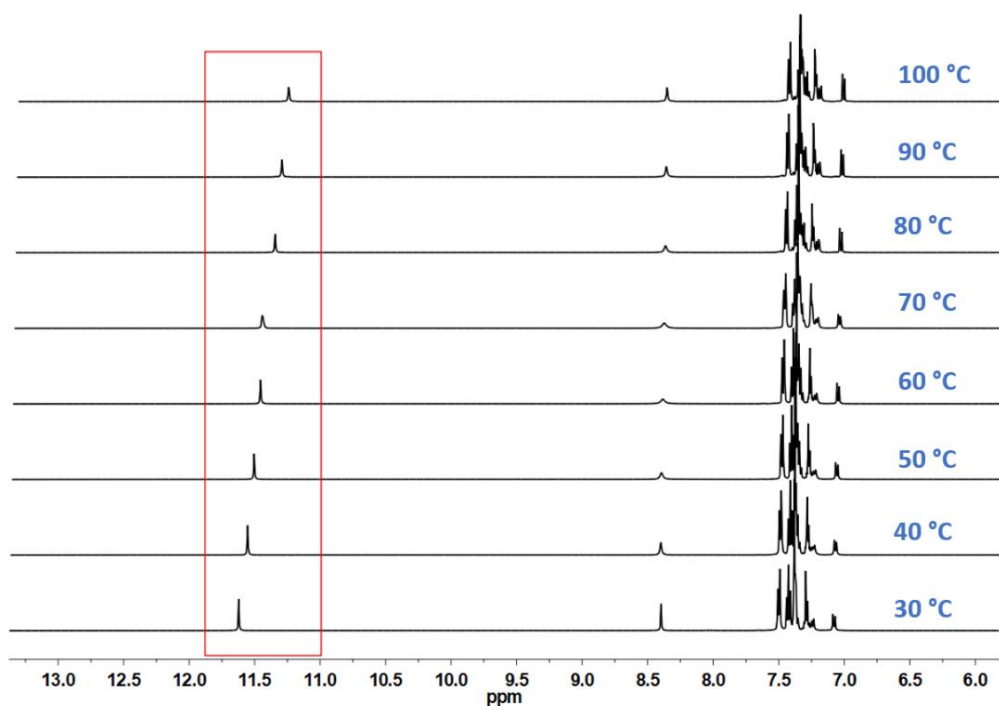


Figure S17. Variable temperature NMR spectra of D1 in DMSO- d_6 from $30\text{ }^{\circ}\text{C}$ to $100\text{ }^{\circ}\text{C}$

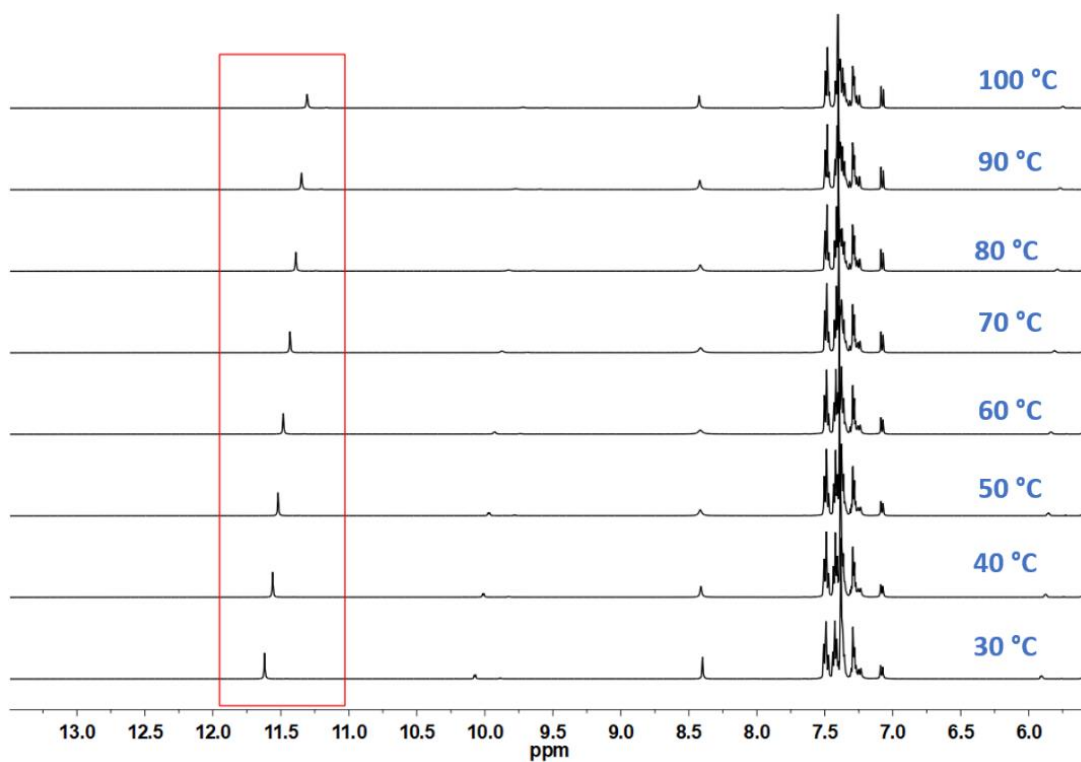


Figure S18. Variable temperature NMR spectra of D2 in DMSO-d₆ from 30 °C to 100 °C.

Table S19. Entrapment and loading efficiency of D2 nanomicelles

Dox (mg)	D2 (mg)	Drug / Dendrimer (w/w)	Entrapment %	Loading %
5	10	1:2	10.6 ± 3.2	5.3 ± 1.6
10	10	1:1	20.3 ± 1.8	20.6 ± 1.8
20	10	2:1	34.7 ± 2.8	69.4 ± 4.8
30	10	3:1	41.5 ± 3.2	70.5 ± 3.4

Table S20. Results and the equation parameters for the release kinetic of Doxorubicin drug from D2-Dox

	Model	Equation	k (h ⁻¹)	n	R^2	No of parameters	$\overline{R^2}$
Free dox	First order	$Q_t = Q_0 e^{-kt}$	0.052	-	0.988	1	0.988
	Korsmeyer - Peppas	$\frac{M_t}{M_\infty} = kt^n$	13.490	0.486	0.966	2	0.965
D2-Dox	First order	$Q_t = Q_0 e^{-kt}$	0.0145	-	0.770	1	0.769
	Korsmeyer - Peppas	$\frac{M_t}{M_\infty} = kt^n$	7.934	0.450	0.977	2	0.976

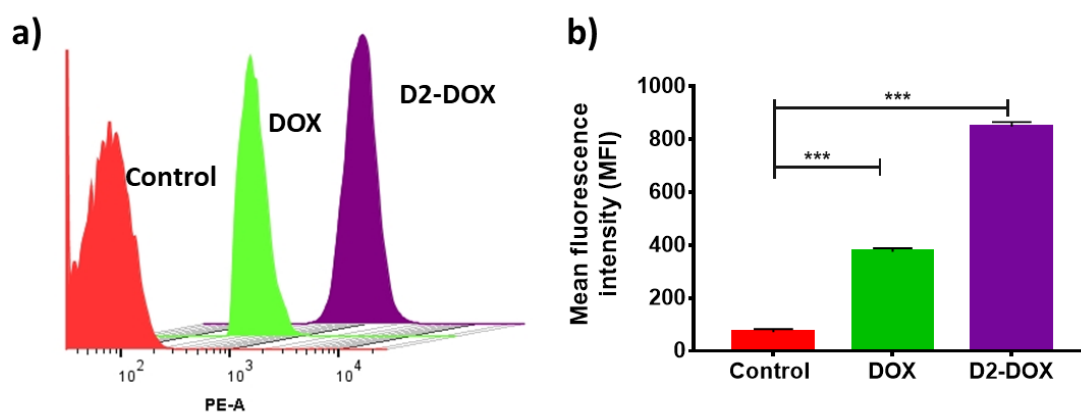


Figure S22: Flowcytometric analysis of the D2-Dox and Dox on a) NIH/3T3 cells incubated for 4 h; b) Mean fluorescence intensity of the internalized D2-Dox and free Dox in NIH/3T3 cells for 4 h;

References:

- 1 P. Rajamalli, P. S. Sheet and E. Prasad, *Chem. Commun. (Camb)*., 2013, **49**, 6758–60.
- 2 N. V. Mulye and S. J. Turco, *Drug Dev. Ind. Pharm.*, 1995, **21**, 943–953.
- 3 N. A. Peppas and J. J. Sahlin, *Int. J. Pharm.*, 1989, **57**, 169–172.
- 4 P. Costa and J. M. Sousa Lobo, *Eur. J. Pharm. Sci.*, 2001, **13**, 123–133.
- 5 R. W. Korsmeyer, R. Gurny, E. Doelker, P. Buri and N. A. Peppas, *Int. J. Pharm.*, 1983, **15**, 25–35.
- 6 M. Ferrari, M. C. Fornasiero and A. M. Isetta, *J. Immunol. Methods*, 1990, **131**, 165–72.